Genomics driven metabolomics novel strategies for the discovery and identification of secondary metabolites

Ries, M.

Chapter 3

Novel key metabolites reveal further branching of the roquefortine/meleagrin biosynthetic pathway

Based on

Marco I. Ries*, Hazrat Ali*, Peter P. Lankhorst, Thomas Hankemeier, Roel A.L. Bovenberg, Arnold J.M. Driessen, Rob J. Vreeken
Novel key metabolites reveal further branching of the roquefortine/meleagrin biosynthetic pathway
Submitted for publication

** these authors contributed equally*

Abstract

Metabolic profiling and structural elucidation of novel secondary metabolites obtained from derived deletion strains of the filamentous fungus Penicillium chrysogenum were used to reassign various previously ascribed synthetase genes of the roquefortine/meleagrin pathway to their corresponding products. Next to the structural characterization of roquefortine F and neoxaline, which are for the first time reported for P. chrysogenum, we identified three novel metabolites, namely roquefortine L, M and N which harbor remarkable chemical structures. Their biosynthesis is discussed, questioning the exclusive role of glandicoline A as key intermediate in the pathway. The results reveal that further enzymes of this pathway are rather unspecific and catalyze more than one reaction leading to excessive branching in the pathway with meleagrin and neoxaline as end products of two branches.

Introduction

The filamentous fungus Penicillium chrysogenum is commercially exploited for many decades due to its high production of β-lactam antibiotics like penicillin G (Weber, et al., 2012). Next to penicillins, secondary metabolites like roquefortines and glandicolines were isolated from liquid cultures of P. chrysogenum which show pharmaceutically interesting properties, like neurotoxic (Scott, et al., 1976), antimicrobial (Clark, et al., 2005; Koolen, et al., 2012) and antitumor (Du, et al., 2010) activities. They are structurally closely related and arise from the roquefortine/meleagrin pathway which contains a di-modular Non-Ribosomal Peptide Synthetase (NRPS) flanked by six associated genes (Ali, et al., 2013; Garcia-Estrada, et al., 2011). Starting with histidyltryptophanyldiketopiperazine (HTD), synthesized by the core synthetase enzyme RoqA using tryptophan and histidine as substrates, RoqD catalyzes the reversed prenylation of HTD at the C-3 of its indole moiety utilizing dimethylallyldiphosphate to form roquefortine D. At the same time, RoqR, a cytochrome p450 oxidoreductase, oxidizes HTD at its histidinyl moiety to dehydrohistidyltryptophanyldiketo-piperazine (DHTD). Both simultaneous reactions of HTD lead to a branch of the roquefortine/meleagrin pathway, one to DHTD via the oxidation by RoqR and further to roquefortine C by dimethylallyl addition of RoqD, and the other via an alteration of the enzymatic order. There, dimethylallyl addition is first performed by RoqD to yield roquefortine D while further oxidation is carried out by RoqR yielding roquefortine C (Figure 1). Although several labeling, silencing and deletion experiments have been conducted, there is still ambiguity about the subsequent biosynthetic reactions and the genes involved. For instance, roquefortine C is supposed to be converted into glandicoline A and further to glandicoline B with RoqM and RoqO each catalyzing one reaction (Ali, et al., 2013; Garcia-Estrada, et al., 2011). However, their assignment to a particular reaction is still unclear. In addition, neoxaline was proposed as final product of the pathway, originating from a hydrogenation of meleagrin (Overy, et al., 2005), yet no gene could be found in the roq gene cluster performing that reaction.
Here we describe the quantification, structural identification and biosynthesis of five previously unidentified metabolites, obtained from high sensitive comparative metabolite profiling of host and deletion strains. Roquefortine F and neoxaline, next to the three structurally novel metabolites, which we named roquefortine L, M and N, were found to be derived from the roquefortine/meleagrin pathway. These results demonstrate a further branching of this secondary metabolite pathway yielding a variety of intermediates with complex structures and a diverse range of activities.

Experimental procedures

Host strains, media, grown condition and plasmid construction
P. chrysogenum strain DS54555, which lacks both the penicillin cluster genes and the ku70 gene, was used as a host strain for deletion analysis and was kindly supplied by DSM Anti-infective (Delft, the Netherlands). All the strains were grown on YGG-medium for protoplasts formation and transformation. For analysis, cells were grown on SMP medium (glucose, 5.0 g/L; lactose, 75 g/L; urea, 4.0 g/L; Na_2SO_4, 4.0 g/L; CH_3COONH_4, 5.0 g/L; K_2HPO_4, 2.12 g/L; KH_2PO_4, 5.1 g/L) for secondary metabo-

lites production using a shaking incubator at 200 rpm for 168 hours at 25°C.

Metabolite profiling
All strains used for gene assignments were grown in quintuplicate to increase statistical power, according to the procedure described above. Sample preparation was carried out as described previously (Ali, et al., 2013). Metabolomic profiling was performed on an Agilent 1200 Capillary pump (Agilent, Santa Clara, CA) coupled to a Surveyor PDA detector (Thermo Scientific, San Jose, CA) and LTQ-FT-ICR-Ultra mass spectrometer (Thermo Scientific, San Jose, CA) equipped with an ElectroSpray Interface as described earlier (Ali, et al., 2013).

Metabolite identification
The identity of compound **10** was confirmed by comparing retention time and MS fragmentation spectra to its commercially available standard, purchased from Bio-Connect (Huissen, the Netherlands). Compound **6**, **9**, **11** and **12** were identified using NMR after extraction from liquid cultures. **6** was extracted from the *roqN* deletion strain culture filtrate which was made alkaline with 25 % ammonium hydroxide (pH 10) and extracted with dichloromethane. The alkaline dichloromethane layer was evaporated to dryness, redissolved in water containing 50 % acetonitrile, vortexed, centrifuged and transferred to an autosampler vial for fraction collection via preparative reversed phase LC on an Atlantis T3 column (10 x 100mm, 5 µm) (Waters Milford, MA). Compound **9** was extracted following the isolation procedure above except using culture filtrate of the *roqO* deletion strain, while **11** and **12** were obtained from the same culture filtrate after lyophilization and extraction using methanol. The methanol layer was evaporated to dryness, redissolved in water, vortexed, centrifuged and subjected to repeated semi-preparative chromatography as described above. Elemental composition of compounds **6**, **9**, **11** and **12** was determined using high-resolution MS. NMR spectra were recorded on a Bruker Avance III 700 MHz or 600 MHz spectrometer with sample temperatures ranging from 260 K to 300 K, depending on the particular requirements for each sample. By choosing an optimal aquisation temperature, severe line broading could be avoided which was observed for various signals due to conformational averaging. For aquisition, samples were dissolved in equal amounts of DMSO and $CDCl_3$.

*Chemical stability of compound **6***
An aqueous solution of compound **6** was adjusted to pH 2.5 by addition of formic acid. Metabolite profiling was carried out as described above. Products, formed by a degradation of **6**, were compared to extracted standards using HPLC-MS/MS.

Results

Metabolite profiling of host and deletion strains leads to five new metabolites of the roquefortine/meleagrin pathway
In a previous study, we described the identification of various abundant metabolites and resolved the major enzymatic steps belonging to the roquefortine/meleagrin pathway (Ali, et al., 2013). In order to identify secondary metabolites originating from the *roq* gene cluster (Figure 1A), culture supernatants of the host strain and

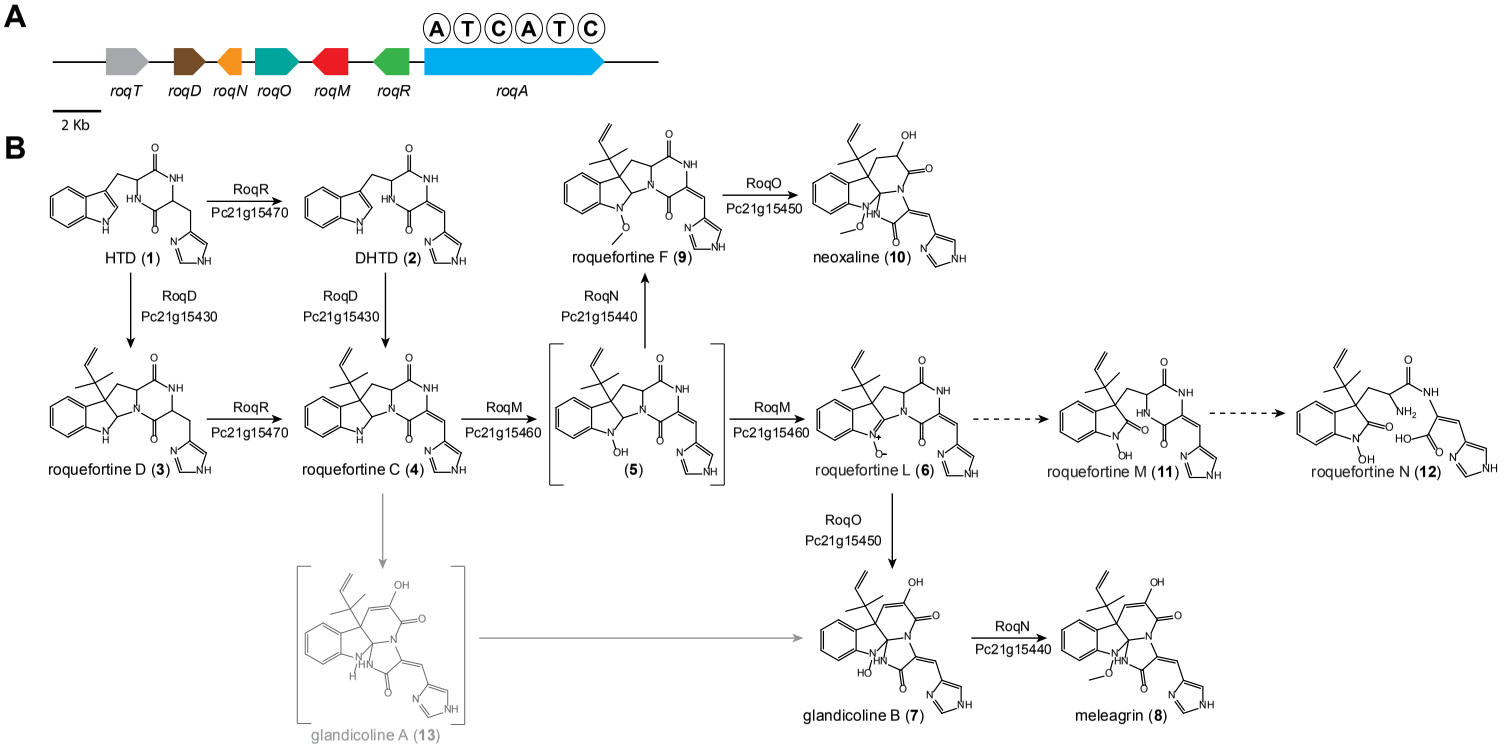

Figure 1. Roquefortine/meleagrin biosynthetic gene cluster and proposed corresponding pathway.
(A) Organization of the roquefortine/meleagrin biosynthetic gene cluster. (B) Proposed roquefortine/meleagrin pathway. Numbers between brackets are compound identifiers used throughout the manuscript. Enzymatic catalyzed reactions are indicated by solid arrows whereas chemical reactions are indicated by dashed arrows. Structures shown in brackets could not be detected whereas grey colored reactions and compounds were previously proposed for various Penicillium species (Garcia-Estrada, et al., 2011; Overy, et al., 2005; Vinokurova, et al., 2002).

individually *roq* gene deletion strains were subjected to comparative metabolite profiling using HPLC-UV-MS (Figure 2). As host strain, *P. chrysogenum* DS54555 was used which is derived from the industrial DS17690 strain lacking the *ku70* gene and multiple penicillin biosynthetic genes clusters. Here, we describe the identification and quantification of several less abundant metabolites, roquefortine L (**6**), roquefortine F (**9**), neoxaline (**10**), roquefortine M (**11**) and roquefortine N (**12**) (Figure 1B) that have not been previously considered or structurally characterized, filling missing biosynthetic reaction steps in the roquefortine/meleagrin pathway.

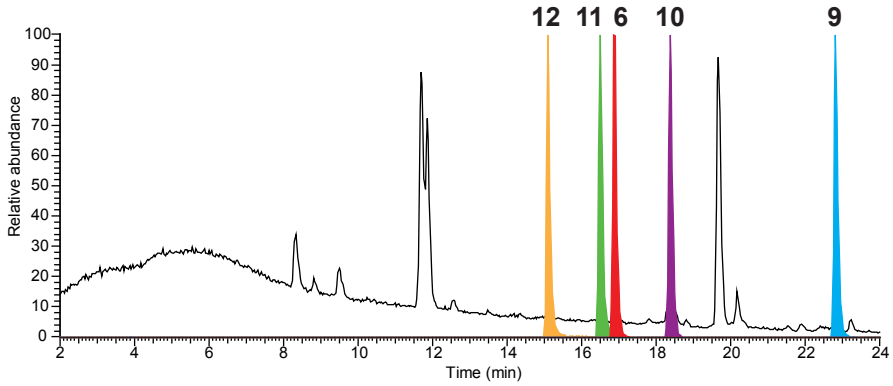

Figure 2. HPLC-MS elution profiles of novel metabolites of the meleagrin/neoxaline pathway.
HPLC-MS total ion chromatogram (TIC, black) and normalized extracted ion chromatograms (EIC, colored) of novel secondary metabolites from the meleagrin/neoxaline pathway. Roquefortine N (**12**, 15.1 min), roquefortine M (**11**, 16.5 min), roquefortine L (**6**, 16.8 min), neoxaline (**10**, 17.8 min), and roquefortine F (**9**, 22.8 min).

*Structure elucidation and quantification of **6**, **11** and **12***

Compound **6** is a novel complex metabolite composed of a roquefortine scaffold and a rare nitrone moiety, thus named roquefortine L. The mass-to-charge ratio of its corresponding ion was observed at 404.1706 using HPLC-FT-ICR-MS, representing the protonated molecule $[M+H]^+$ with formula $C_{22}H_{22}N_5O_3$ (calc. 404.1717) eluting at 16.5 minutes. The same ion was previously tentatively identified as glandicoline A (**13**) (Figure 1B), as elemental composition and parts of the structure indicated consistency with this compound (Ali, et al., 2013). However, its ^{1}H- and ^{13}C-NMR data showed high similarity to the diketopiperazine **4**, indicating a roquefortine-like core structure. Furthermore, its ^{1}H-NMR spectrum revealed two protons at C-8 representing a single bond between C-8 and C-9, which is different from the double bond described for **13** (Supplemental Figure 1, Supplemental Table 1). Additionally, C-2 (δ_C = 146) in the ^{13}C-HMBC spectrum indicated a double bond between N-1 and C-2 which was supported by the chemical shift of N-1 (δ_N = 280) in the ^{15}N-HMBC spectrum (Supplemental Figure 2, Supplemental Table 1). As compound **13** was reported from various *Penicillium* species like *P. albocoremium* (Overy, et al., 2005), *P. glandicola* (Kozlovskii, et al., 1994) and *P. chrysogenum* (Vinokurova, et al., 2002) and proposed as a precursor of **7**, host and *roq* deletion strain chromatograms of *P. chrysogenum* were further analyzed for the presence of **13**. The chromatogram of the ion with *m/z* 404.1706, representing the protonated molecular $[M+H]^+$ with formula $C_{22}H_{22}N_5O_3$ of both compounds **6** and **13**, was extracted in a 5 ppm mass

accuracy window. However, no ion possibly corresponding to **13** could be found whereas **6** was observed at high concentration in the liquid media (Figure 3).

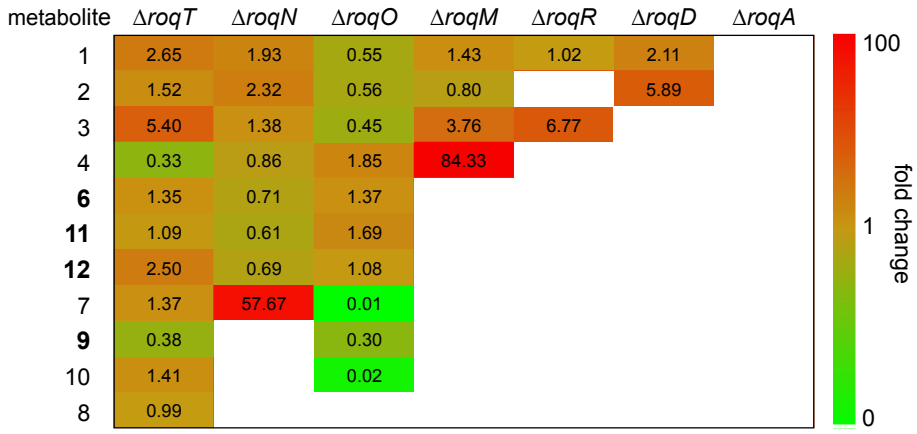

Figure 3. Fold change of the concentration of secondary metabolites from the roquefortine/meleagrin pathway in deletion strains compared to the host strain.
Numbers in table represent the internal standard corrected concentrations of secondary metabolites in supernatants of deletion strains obtained from HPLC-UV-MS compared to their concentration in the supernatant of the host strain *P. chrysogenum* DS54555. Cell coloring, representing the fold change, was performed on a logarithmic scale. Red colored cells indicate a concentration increase whereas green colored cells represent a decrease. Cells colored in white indicate a complete absence of the metabolite in the deletion sample. Novel metabolites of the roquefortine/meleagrin pathway are shown with bold numbers.

The absence of **13** in host and various *P. chrysogenum* strains lead to the conclusions that **13** is not produced by *P. chrysogenum* DS54555.
Compound **11** and **12** are novel compounds based on a roquefortine-like scaffold, thus named roquefortine M and roquefortine N. HR-ESI-MS of **11** (*m/z* 422.1814 $[M+H]^+$, calc. 422.1824) and **12** (*m/z* 440.1918 $[M+H]^+$, calc. 440.1928) established the molecular formula $C_{22}H_{23}N_5O_4$ and $C_{22}H_{25}N_5O_5$. Their chemical structure was determined using ^{13}C-HMBC, ^{15}N-HMBC and ^{1}H-NMR (Supplemental Figure 3 and 4, Supplemental Table 2) showing similar signals as observed for compound **6**, which indicates a similar chemical scaffold. However, the significant upfield shift of N-1 (from δ_N = 280 in **6** to δ_N = 185 in **11**) in the ^{15}N-HMBC spectra together with the chemical shift of C-2 (δ_C = 146 in **6**, δ_C = 172 in **11**) in the ^{13}C-NMR spectra of compound **11** shows that **11** contains a single bond between N-1 and C-2, with C-2 being a carbonylic carbon. In addition, a comparison between the ^{15}N-HMBC spectrum of compound **11** and **12** revealed that the amide-bond between N-14 and C-13 in **11** was hydrolyzed in **12** (δ_N = 32.0) yielding a primary amine and a carboxyl group. Both compounds commonly occur, together with compound **6**, in liquid cultures of *P. chrysogenum* host and *roqT*, *roqN* and *roqO* deletion strains (Figure 3). Their absence in the remaining deletion strain samples concludes the involvement of *roqA*, *roqR*, *roqD* and *roqM* in their biosynthesis.

*Structure elucidation and quantification of **9** and **10***
Compound **9** with molecular formula $C_{23}H_{25}N_5O_3$, established by HR-ESI-MS (*m/z*

420.2015 $[M+H]^+$, calc. 420.2030), was identified as roquefortine F, a metabolite solely reported from a deep-ocean sediment derived *Penicillium* species (Du, et al., 2009), using ^{1}H- and ^{13}C-NMR (Supplemental Figure 5, Supplemental Table 3). Its ^{1}H-NMR spectrum is very similar to the spectrum of **3** (Ali, et al., 2013), except a double bond between C-12 and C-15. Furthermore, the presence of C-26 (δ_C = 63.6) in the ^{13}C-NMR spectrum, next to a sharp OCH_3 peak (δ_H = 4.01) and a missing proton on N-1 in the ^{1}H-NMR spectrum fully agree with a methoxylated N-1 in compound **9**. This was supported by the absence of correlations with a carbon or proton in the HMBC spectrum. The concentration of **9**, particularly high in the host strain, was found to be reduced to approximately one third in the deletion strains of *roqT* and *roqO* and absent in the remaining deletion strains (Figure 3). This data suggest that *roqO* and *roqT* are the only two genes not involved in the biosynthesis of **9**. Compound **10** with molecular formula $C_{23}H_{25}N_5O_4$ (*m/z* 436.1967 $[M+H]^+$, calc. 436.1979) was identified as neoxaline, a metabolite previously isolated from *Aspergillus japonicas* Fg-551 (Hirano, et al., 1979) and *P. tulipae* (Overy, et al., 2006), by comparing retention time and MS/MS fragments to its commercially available standard (Supplemental Figure 6). While the concentration of **10** in host and *roqT* deletion strain is almost comparable, a 97% decrease was observed in the *roqO* deletion strain (Figure 3). In all remaining deletion strains, compound 10 could not be detected leading to the conclusion that all genes in the *roq* gene cluster, except *roqT*, are required for the synthesis of **10**.

*Chemical degradation of compound **6** leads to various products*

Nitrones, such as compound **6**, are not infinitely stable and degrade already at room temperature in aqueous solution as well as under acidic conditions by incorporation of water (Cashman, et al., 1999; Rodriguez, et al., 1999; Sun, et al., 2007). In order to determine the resulting degradation products, an aqueous solution of **6** was acidified and the resulting sample measured using HPLC-UV-MS (Figure 4). Next to a 50 % decrease of **6**, two highly abundant ions were observed in the treated sample corresponding to **11** and **12**. Additionally a third unidentified compound was found eluting at 17.33 minutes with a mass-to-charge ratio of 422.1823, representing the protonated molecule with the formula $C_{22}H_{24}N_5O_4$. These results demonstrate that **11**, **12** and an unidentified third compound are produced by degradation of the rather unstable compound **6**.

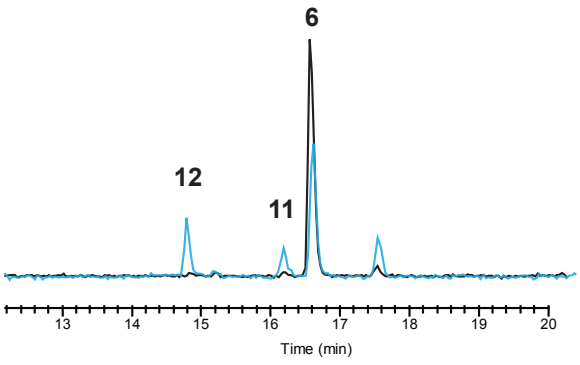

Figure 4. Chemical degradation of compound **6** leads to various products.
Total ion chromatogram of pure (black) and degraded compound **6** (blue) after addition of formic acid measured on HPLC-MS. Acid induced degradation leads to the formation of **11** and **12** next to an unidentified compound eluting at 17.33 minutes with $[M+H]^+$= 422.1823 and elemental composition $C_{22}H_{23}N_5O_4$.

Discussion

Here, we present new insight into the complex biosynthesis of secondary metabolites from the roquefortine/meleagrin pathway. Five novel metabolites were found to originate from the *roq* gene cluster, obtained from comparative metabolites profiling of the host strain and various deletion strains in combination with NMR and MS based structure elucidation. As all five metabolites are produced in a late stage of the pathway, no changes were observed for the biosynthesis of upstream metabolites **1** – **4**, which starts with RoqA taking L-histidine and L-tryptophan as substrates and producing compound **1**. Based on the highly significant accumulation of **4** in the *roqM* deletion strain and the absence of all downstream metabolites **6** – **12** (Figure 3), it can be concluded that *roqM*, encoding a flavin-dependent MAK 1-monooxygenase like protein, is involved in the conversion of **4** into **6**, a novel compound containing an unusual nitrone moiety. Nitrones are widely known due to their free radical trapping properties and their potential application as therapeutics in age related diseases (Floyd, et al., 2008) like cancer (Floyd, et al., 2011) and ischaemic stroke (Maples, et al., 2004). As the chemical scaffold of compound **6** is closely related to the roquefortine group it was named roquefortine L. Flavin-containing monooxygenases are commonly known to consecutively oxidize drugs and xenobiotics containing a soft-nucleophile, such as nitrogen or sulfur (Krueger and Williams, 2005). In case of secondary amines, flavin-containing monooxygenases consecutively oxidize the nitrogen, leading to the production of hydroxylamines and nitrones (Cashman, et al., 1999; Rodriguez, et al., 1999; Sun, et al., 2007). A similar mechanism for the synthesis of the nitrone containing compound **6** is very likely, starting with the oxidation of the secondary amine in the indole part of **4**, yielding the hydroxylated intermediate **5** (Figure 5). Further oxidation on the same

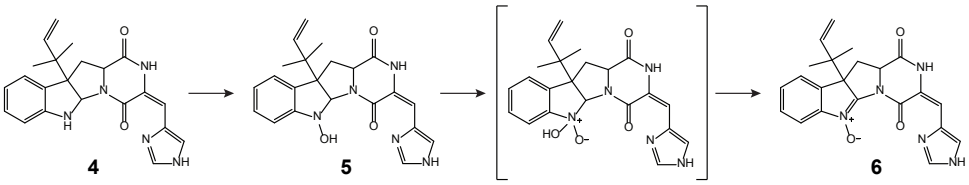

Figure 5. Proposed biosynthesis of **6** by RoqM.

nitrogen produces an unstable N,N-dihydroxylated species which is followed by the loss of water, producing eventually compound **6**. However, nitrones are not indefinitely stable and easily degrade at room temperature in aqueous solutions (Cashman, et al., 1999; Rodriguez, et al., 1999; Sun, et al., 2007). Under acidic conditions compound **6** decomposes by a consecutive incorporation of water leading, among others, to the production of compound **11** and **12** (Figure 4 and 6). This decomposition was also observed in NMR experiments after extended storage of a solution of 6 at room temperature. These results suggest that the presence of **11** and **12** in liquid cultures of *P. chrysogenum* can be attributed to a chemical degradation of **6**. Compound **6**, with the formula $C_{22}H_{21}N_5O_3$, is represented by an ion with a mass-to-charge ratio of 404.1706 and eluting at 16.8 minutes. The exact same ion was

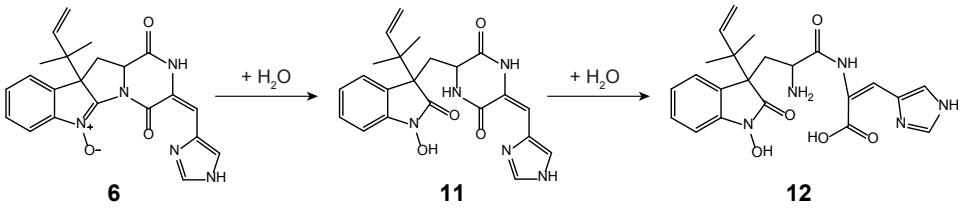

Figure 6. Degradation of **6** yielding **11** and **12** by consecutive incorporation of water.

previously tentatively identified as compound **13** (Ali, et al., 2013) as its elemental composition and parts of the structure indicated consistency with this compound. However, further structure elucidation using various NMR experiments confirmed the structure of **6** instead. This was surprising as compound **13**, a proposed key-intermediate in the biosynthesis of downstream metabolites like **7**, **8** and **10** was previously tentatively identified in different *Penicillium* cultures (Overy, et al., 2005; Vinokurova, et al., 2002). By using a comparable instrumental set-up with a similar chromatographic separation method, host and deletion strains of DS54555 were screened for production of **13**. Nevertheless, neither **13** nor corresponding degradation products could be detected, whereas **6** was found at high concentrations leading to the conclusion that **13** is not produced by *P. chrysogenum*. This is remarkable as **13** was expected as single precursor of **7**, modified by RoqO (Garcia-Estrada, et al., 2011). In addition, a deletion of *roqO* resulted in an up to 98 % decrease of **7** whereas the levels of upstream metabolites remained nearly unchanged, indicating that RoqO is indeed involved in the synthesis of **7**. Due to the general absence of **13** in the *P. chrysogenum* derived samples, compound **7** has to originate from a different biosynthetic route than the previously reported oxidation of **13** on its indole nitrogen (Ali, et al., 2013; Garcia-Estrada, et al., 2011; Overy, et al., 2005). RoqO, encoding a p450 monooxygenase, closely resembles FtmG (64% identity, 79% similarity at the amino acid level) a cytochrome p450 monooxygenase catalyzing the hydroxylation of fumitremorgin C to dihydroxy-fumitremorgin C (Kato, et al., 2009), compounds that are structurally similar to the roquefortine derivatives. A possible deduced biosynthesis of **7** involves the hydroxylation of **6** on C-9 by RoqO similar to the oxidation of fumitremorgin C by FtmG. Subsequent cleavage of the bond between C-9 and N-14 followed by the development of a bond between C-2 and N-11 is postulated to yield ultimately **7**. These results, together with the general absence of **13** in *P. chrysogenum* lead to the conclusion that **7** and **8** are produced via a different biosynthesis in *P. chrysogenum* than in other *Penicillium* strains like *P. tulipae* (Overy, et al., 2005), for which a tentatively identified **13** was reported as intermediate.

The deletion of *roqN* resulted in an accumulation of **7** in the liquid medium whereas metabolites **8**, **9** and **10** were absent (Figure 3). RoqN, a methyltransferase, was previously recognized to catalyze the addition of a methyl group on the hydroxylated nitrogen of **7** producing **8** (Ali, et al., 2013; Garcia-Estrada, et al., 2011). As **9** contains a methylated hydroxylamine group in the same position as **8**, the hydroxylamine containing compound **5**, which differs only in a methyl-group, is proposed as its direct precursor with RoqN catalyzing the methyl addition to yield **9**. These results

reveal a further branching of the roquefortine/meleagrin pathway with compounds **6** and **9** being products of **5**. In addition, they support the presence of **5**, which was proposed based on its involvement in the biosynthesis of **6**.
Compound **10** was previously proposed as direct product of **8** by enzymatic hydrogenation (Overy, et al., 2005). However, BLAST analysis did not reveal an enzyme in the roquefortine/meleagrin pathway, which is able to perform that reaction (Ali, et al., 2013; Garcia-Estrada, et al., 2011). Moreover, a 53 times higher concentration of **8** compared to **10** in the host strain, but the absence of **8** in the *roqO* deletion strain with **10** still being present, leads to the conclusion that **8** is not a precursor of **10** (Figure 3). In contrast, due to the high concentration of **9** in the *ΔroqO* strain and its roquefortine-like structure (roquefortine scaffold with a methoxygroup on N-1), compound **9** is proposed as direct precursor of **10** with RoqO catalyzing this reaction, similar to the synthesis of **7** from **6**. These results suggest that RoqO is involved in the reactions from **6** into **7** and from **9** into **10** by oxidizing and subsequently converting a roquefortine scaffold into a glandicoline like structure (Figure 1B).
In conclusion, these results extend the additional branch of compound **9** leading to the final product **10**. Unspecificity, already observed for RoqR and RoqD (Ali, et al., 2013), could now also be observed for RoqO and RoqN leading to a complex degree of branching in the pathway and a wide palette of compounds. Several of the new compounds identified in the current study were found to be equipped with interesting biological activities. Roquefortine F, previously reported from a deep ocean sediment derived fungus *Penicillium* sp., shows moderate cytotoxicity against various tumor cell lines (Du, et al., 2009). Neoxaline, which was first isolated from *A. japonicas* Fg-551, stimulates the central nervous system in mice (Hirano, et al., 1979) and inhibits cell proliferation (Koizumi, et al., 2004). Furthermore, it was found to induce cell cycle arrest at the G2/M phase in Jurkat cells (inhibition of tubulin polymerization) (Koizumi, et al., 2004). Here, the novel metabolites roquefortine L, roquefortine M and roquefortine N are added to the palette of potential cytotoxic compounds, which demonstrates the potential of engineered industrial *P. chrysogenum* strains to produce novel bioactive compounds with unusual chemical scaffolds.

Acknowledgements

We would like to thank Drs. H. Menke, W. Heijne and H. Roubos from the DSM Biotechology Centre for making the DNA microarray data available.

References

Ali, H., Ries, M.I., Nijland, J.G., Lankhorst, P.P., Hankemeier, T., Bovenberg, R.A., Vreeken, R.J., and Driessen, A.J. (2013). A Branched Biosynthetic Pathway Is Involved in Production of Roquefortine and Related Compounds in Penicillium chrysogenum. PLoS One 8, e65328.

Cashman, J.R., Xiong, Y.N., Xu, L., and Janowsky, A. (1999). N-oxygenation of amphetamine and methamphetamine by the human flavin-containing monooxygenase (form 3): role in bioactivation and detoxication. J Pharmacol Exp Ther 288, 1251-1260.

Clark, B., Capon, R.J., Lacey, E., Tennant, S., and Gill, J.H. (2005). Roquefortine E, a diketopiperazine from an Australian isolate of Gymnoascus reessii. J Nat Prod 68, 1661-1664.

Du, L., Feng, T., Zhao, B., Li, D., Cai, S., Zhu, T., Wang, F., Xiao, X., and Gu, Q. (2010). Alkaloids from a deep ocean sediment-derived fungus Penicillium sp. and their antitumor activities. J Antibiot (Tokyo) 63, 165-170.

Du, L., Li, D., Zhu, T., Cai, S., Wang, F., Xiao, X., and Gu, Q. (2009). New alkaloids and diterpenes from a deep ocean sediment derived fungus Penicillium sp. Tetrahedron 65, 1033-1039.

Floyd, R.A., Chandru, H.K., He, T., and Towner, R. (2011). Anti-cancer activity of nitrones and observations on mechanism of action. Anticancer Agents Med Chem 11, 373-379.

Floyd, R.A., Kopke, R.D., Choi, C.H., Foster, S.B., Doblas, S., and Towner, R.A. (2008). Nitrones as therapeutics. Free Radic Biol Med 45, 1361-1374.

Garcia-Estrada, C., Ullan, R.V., Albillos, S.M., Fernandez-Bodega, M.A., Durek, P., von Dohren, H., and Martin, J.F. (2011). A single cluster of coregulated genes encodes the biosynthesis of the mycotoxins roquefortine C and meleagrin in Penicillium chrysogenum. Chemistry & biology 18, 1499-1512.

Hirano, A., Iwai, Y., Masuma, R., Tei, K., and Omura, S. (1979). Neoxaline, a new alkaloid produced by Aspergillus japonicus. Production, isolation and properties. J Antibiot (Tokyo) 32, 781-785.

Kato, N., Suzuki, H., Takagi, H., Asami, Y., Kakeya, H., Uramoto, M., Usui, T., Takahashi, S., Sugimoto, Y., and Osada, H. (2009). Identification of cytochrome P450s required for fumitremorgin biosynthesis in Aspergillus fumigatus. ChemBiochem 10, 920-928.

Koizumi, Y., Arai, M., Tomoda, H., and Omura, S. (2004). Oxaline, a fungal alkaloid, arrests the cell cycle in M phase by inhibition of tubulin polymerization. Biochim Biophys Acta 1693, 47-55.

Koolen, H.H., Soares, E.R., Silva, F.M., Souza, A.Q., Medeiros, L.S., Filho, E.R., Almeida, R.A., Ribeiro, I.A., Pessoa Cdo, O., Morais, M.O., et al. (2012). An antimicrobial diketopiperazine alkaloid and co-metabolites from an endophytic strain of Gliocladium isolated from Strychnos cf. toxifera. Nat Prod Res 26, 2013-2019.

Kozlovskii, A.G., Vinokurova, N.G., Reshetilova, T.A., Sakharovskii, V.G., Baskunov, B.P., and Seleznev, S.G. (1994). New metabolites of Penicillium glandicola var. glandicola - glandicoline A and glandicoline B. Appl Biochem Microbiol 30, 334-337.

Krueger, S.K., and Williams, D.E. (2005). Mammalian flavin-containing monooxygenases: structure/function, genetic polymorphisms and role in drug metabolism. Pharmacol Ther 106, 357-387.

Maples, K.R., Green, A.R., and Floyd, R.A. (2004). Nitrone-related therapeutics: potential of NXY-059 for the treatment of acute ischaemic stroke. CNS Drugs 18, 1071-1084.

Overy, D.P., Nielsen, K.F., and Smedsgaard, J. (2005). Roquefortine/oxaline biosynthesis pathway metabolites in Penicillium ser. Corymbifera: in planta production and implications for competitive fitness. J Chem Ecol 31, 2373-2390.

Overy, D.P., Phipps, R.K., Frydenvang, K., and Larsen, T.O. (2006). epi-Neoxaline, a chemotaxonomic marker for Penicillium tulipae. Biochem Syst Ecol 34, 345-348.

Rodriguez, R.J., Proteau, P.J., Marquez, B.L., Hetherington, C.L., Buckholz, C.J., and O'Connell, K.L. (1999). Flavin-containing monooxygenase-mediated metabolism of N-deacetyl ketoconazole by rat hepatic microsomes. Drug Metab Dispos 27, 880-886.

Scott, P.M., Merrien, M.A., and Polonsky, J. (1976). Roquefortine and iso-fumigaclavine A, metabolites from Penicillium roqueforti. Experientia 32, 140-142.

Sun, H., Ehlhardt, W.J., Kulanthaivel, P., Lanza, D.L., Reilly, C.A., and Yost, G.S. (2007). Dehydrogenation of indoline by cytochrome P450 enzymes: a novel "aromatase" process. J Pharmacol Exp Ther 322, 843-851.

Vinokurova, N.G., Boichenko, L.V., and Arinbasarov, M.U. (2002). Production of Alkaloids by Fungi of the Genus Penicillium Grown on Wheat Grain. Appl Biochem Microbiol 39, 403-406.

Weber, S.S., Polli, F., Boer, R., Bovenberg, R.A., and Driessen, A.J. (2012). Increased penicillin production in Penicillium chrysogenum production strains via balanced overexpression of isopenicillin N acyltransferase. Appl Environ Microbiol 78, 7107-7113.

Supplemental Information

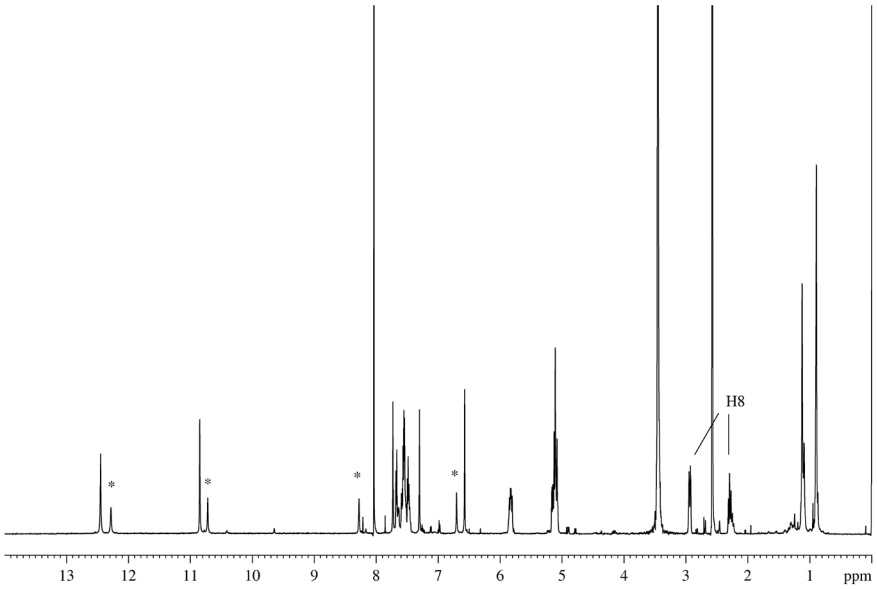

Supplemental Figure 1. ^{1}H-NMR spectrum of roquefortine L (**6**) in DMSO/$CDCl_3$ acquired at 300K on a 600 MHz spectrometer. Small additional peaks labeled with a star correspond to a second conformation of **6**. Assignments can be found in Supplemental Table 1.

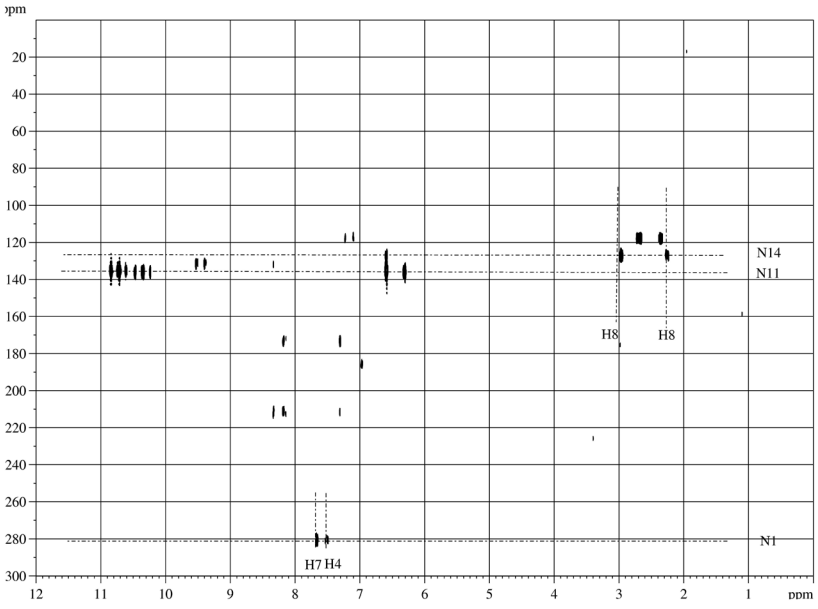

Supplemental Figure 2. ^{15}N-HMBC spectrum of compound **6** acquired at 290 K. Small additional peaks correspond to compound 11 which was produced by slow degradation of **6**. Further assignments can be found in Supplemental Figure 1.

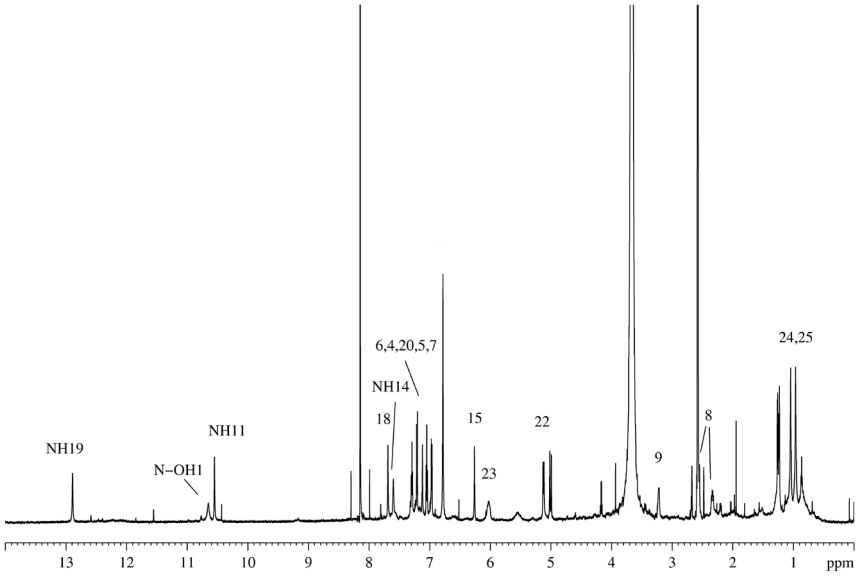

Supplemental Figure 3. ^{1}H-NMR spectrum of roquefortine M (**11**) acquired at 250 K.

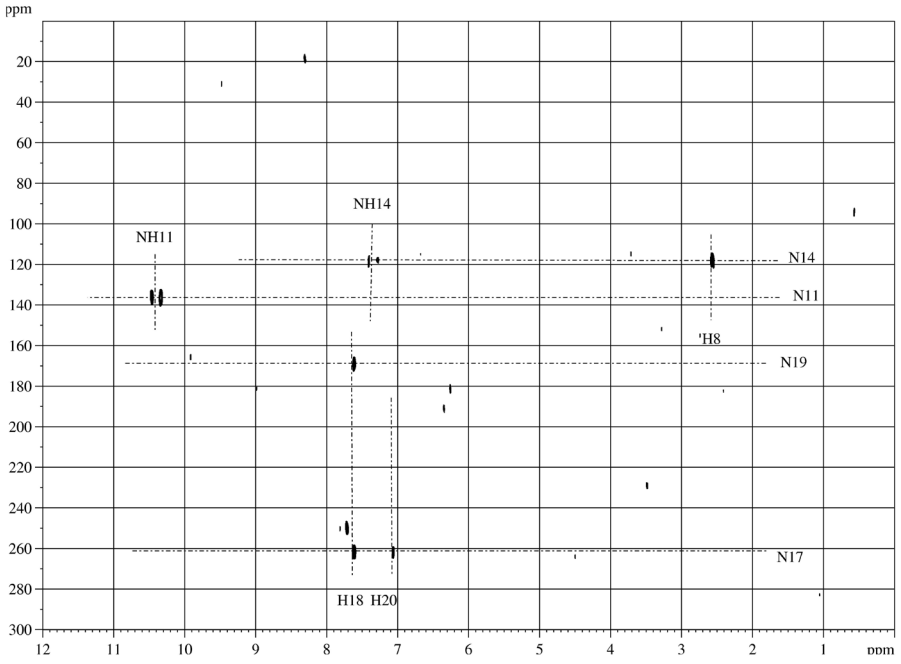

Supplemental Figure 4. ^{15}N-HMBC spectrum of roquefortine M (**11**) acquired at 270 K.

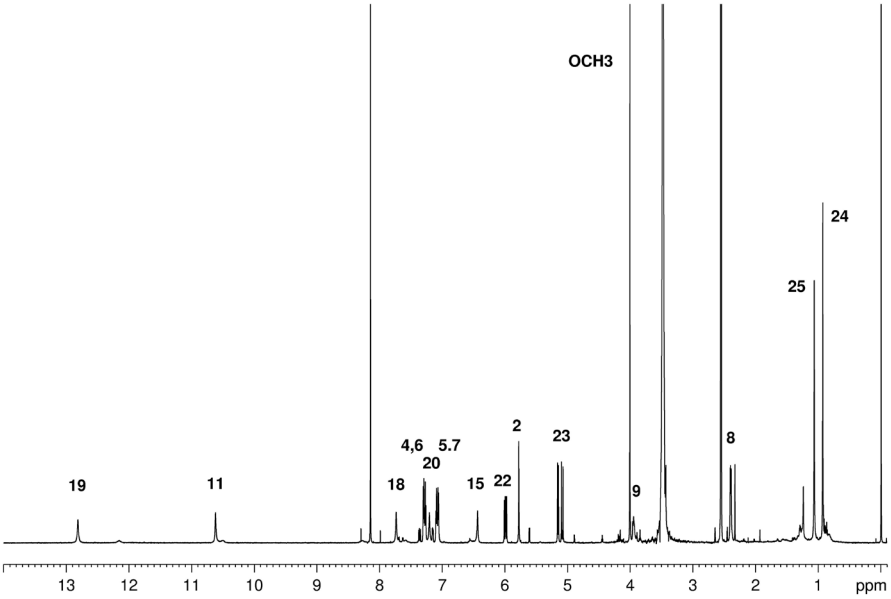

Supplemental Figure 5. ^{1}H-NMR spectrum of roquefortine F (**9**) acquired at 280 K.

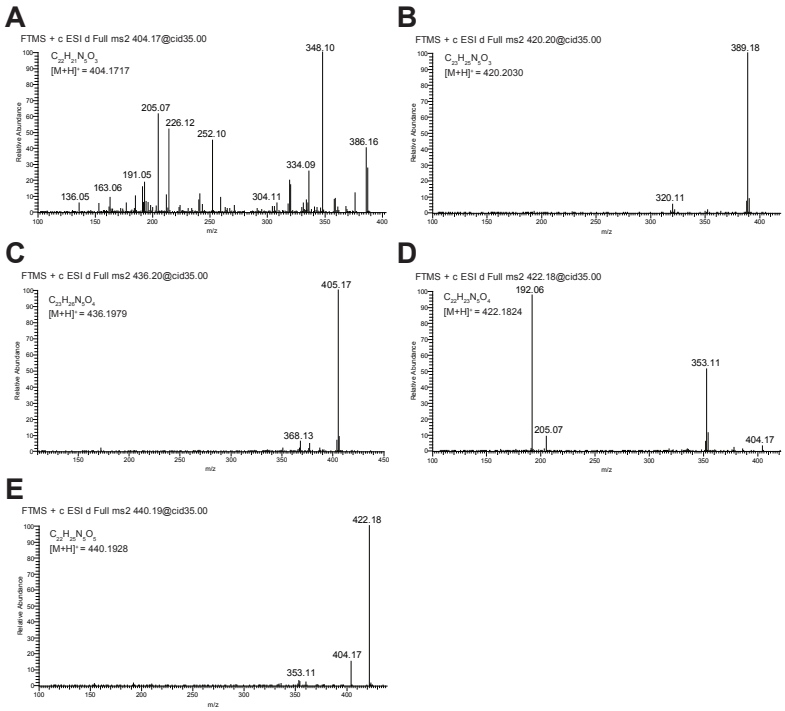

Supplemental Figure 6. HPLC-MS/MS fragmentation spectra including chemical formula and calculated exact mass of metabolites. Metabolites shown are protonated compound **6** (roquefortine L, A), **9** (roquefortine F, B), **10** (neoxaline, C), **11** (roquefortine M, D) and **12** (roquefortine N, E). Spectra were acquired at a LTQ-FT-MS at 35% normalized collision energy in positive ion mode.

roquefortine L (**6**)

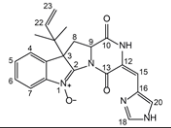

	290 K	280 K	290 K
	δ_H	δ_C	δ_N
1-NO	-		280
2		147.6	
3		58.2	
3a		137.9	
4	7.49	124.3	
5	7.44	129.0	
6	7.52	128.6	
7	7.56	114.9	
7a		148.5	
8	2.24, 2.95	24.5	
9	5.06	63.6	
10		164.9	
11-NH	10.77		136
12		122.2	
13		156.7	
14-N			127
15	6.57	112.2	
16		124.3	
17-N			*
18	7.76	136.3	
19-NH	12.42**		*
20	7.49	132.1	
21		43.1	
22	5.79	141.5	
23	5.06, 5.09	116.2	
24	0.86	22.4	
25	1.09	22.3	

(*) not observed
(**) from spectrum at 280 K

Supplemental Table 1
Chemical shifts of ^{1}H, ^{13}C and ^{15}N-NMR of roquefortine L (**6**) (δ in ppm).

roquefortine M (**11**)

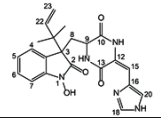

roquefortine N (**12**)

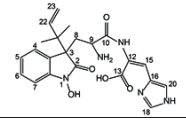

	270K	300K	270K		280K	280K	300K
	δ_H	δ_C	δ_N		δ_H	δ_C	δ_N
1-NOH	10.56		185***		10.64**		*
2		172.6				173.1	
3		65.9				54.5	
3a		124.7				124.7	
4	7.20	125.1			7.18	125.0	
5	7.02	121.6			6.99	121.1	
6	7.27	128.2			7.22	127.6	
7	6.95	106.8			6.93	106.4	
7a		142.9				142.7	
8	2.32, 2.60	35.6			2.09, 2.58	35.0	
9	3.20	52.3			2.74	52.6	
10		165.1				*	
11-NH	10.44		137		10.08**		*
12		121.0				*	
13		160.1				*	
14-NH	7.38		118	14-NH_2	6.57**		30
15	6.26	108.7			8.02	107.1	
16		125.3				127.7	
17-N			262				*
18	7.65	136.4			8.00	133.4	
19-NH	12.87		169		*		196
20	7.09	133.8			7.18	127.6	
21		41.9				41.7	
22	6.00	142.3			6.03	142.5	
23	4.98, 5.09	113.9			4.98, 5.09	113.4	
24	1.04	21.7			1.07	21.4	
25	0.96	21.3			0.98	21.2	

(*) not observed
(**) tentative assignment
(***) from spectrum at 290 K

Supplemental Table 2
Chemical shifts of ^{1}H, ^{13}C and ^{15}N-NMR of roquefortine M (**11**) and roquefortine N (**12**) (δ in ppm).

roquefortine F (**9**)

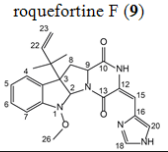

	280K	280K
	δ_H	δ_C
2	5.78	84.9
3		60.5
3a		130.5
4	7.30	124.5
5	7.09	124.4
6	7.27	128.8
7	7.06	116.0
7a		150.9
8	2.40	37.7
9	3.96	57.4
10		164.5
11-NH	10.63	
12		*
13		157.4
14-N14		
15	6.44	109.1
16		*
18	7.75	136.9
19-NH	12.82	
20	7.21	134.2
21		40.5
22	5.99	143.1
23	5.09, 5.16	114.6
24	0.94	23.2
25	1.07	22.4
26	4.01	63.6

(*) not observed

Supplemental Table 3
Chemical shifts of ^{1}H and ^{13}C-NMR of roquefortine F (**9**) (δ in ppm).